Walking Speed Estimation Using a Shank-Mounted Inertial Measurement Unit

Q. Li[*,a,b], M. Young[c], V. Naing[c], J.M. Donelan[c]

[a]*Department of Mechanical and Materials Engineering, Queen's University, Kingston, ON, Canada*
[b]*Human Mobility Research Centre, Queen's University and Kingston General Hospital, Kingston, ON, Canada*
[c]*Department of Biomedical Physiology and Kinesiology, Simon Fraser University, Burnaby, BC, Canada*

Abstract

We studied the feasibility of estimating walking speed and slope using a shank-mounted inertial measurement unit. Our approach took advantage of the inverted pendulum-like behavior of the stance leg during walking to identify a new method for dividing up walking into individual stride cycles and estimating the initial conditions for the direct integration of the accelerometer and gyroscope signals. To test its accuracy, we compared speed and slope estimates to known values during walking overground and on a treadmill. While the slope estimation method systematically underestimated slope, the speed estimation method worked well across treadmill speeds and slopes yielding a root mean square speed estimation error of only 7%. It also worked well during overground walking with a 4% error in the estimated travel distance. This accuracy is comparable to that achieved from foot-mounted sensors, providing an alternative in sensor positioning for walking speed estimation. Shank mounted sensors may be of great benefit for estimating speed in walking with abnormal foot motion and for the embedded control of knee-mounted devices such as prostheses and energy harvesters.

Key words: Gait analysis, Inertial measurement unit, Ambulatory system, Gait cycle, Walking speed, Inverted pendulum model

1. INTRODUCTION

An important component of gait analysis is the determination of walking's spatial and temporal parameters including heel strike, toe-off, cadence, stride length and walking speed. These parameters are useful for diagnosing abnormal gait, evaluating the effectiveness of rehabilitation techniques, monitoring the performance of exercise programs, and providing fall risk indicators [3, 11, 14, 18]. To bring gait analysis out of the laboratory and make it portable, recent efforts have focused on estimating gait parameters using accelerometers and gyroscopes. As the name suggests, an accelerometer is a device for measuring accelerations, including those induced by gravity. A gyroscope measures angular velocity. The combinations of these sensors are referred to as inertial measurement units (IMU). Most studies using accelerometers and gyroscopes have been concerned with estimating temporal gait parameters—such as stride frequency-from characteristic features in the sensor signals when attached to different body locations including the trunk, thigh, shank and foot [16, 2, 10, 17].

Determining walking speed requires estimating stride length in addition to stride frequency. One approach estimates stride length indirectly by first computing an intermediate kinematic parameter from sensor measurements and then relating the stride length to the intermediate parameter using an anthropomorphic model. For example, Miyazaki [15] integrated angular velocity measured by a thigh-mounted gyroscope to determine thigh angle. A single element model related thigh angle to stride length resulting in an error in estimated speed of less than 15%. Aminian et al. [1] used a more realistic two-segment model with gyroscopes mounted on the thigh and shank and achieved a root mean

[*]Corresponding author. Tel:+1-613-533-3191;Fax:+1-613-533-6489.
E-mail address: qli@me.queensu.ca

square estimation error of 7%. (It is only possible to make rough comparisons of measured error between studies because different investigators have used different experimental conditions and calculated error in different ways.) Instead of attaching sensors to the lower limb, Zijlstra and Hof [21] studied the feasibility of estimating spatio-temporal gait parameters using a trunk-mounted accelerometer. From the measured upward and downward displacements of the trunk, an inverted pendulum model estimated mean step length yielding root mean square speed estimation errors ranging from 5% at a walking speed of 0.5 m/s to 14% at a walking speed of 1.75m/s. While these studies demonstrate reasonable accuracy in estimating speed, they are limited by their requirement of subject-specific calibration—the same angles in a taller person will correspond to longer stride lengths and faster speeds.

Instead of estimating spatial parameters indirectly, an alternative is to determine displacements by direct time integration of measured accelerations. This approach is more general than the previously described indirect approach as it does not require subject-specific calibration. It can be more difficult, however, to get accurate results from double time integration of accelerometer measurements. The first issue is that the measured accelerations have contributions not only from the motion of the limb but also from gravity. Gravitational acceleration must be subtracted before integration requiring continuous knowledge of the device angle with respect to gravity—an angle that is often difficult to determine. A second issue is that drift in the accelerometer offset, even if it is very small, can quickly cause large inaccuracies in the estimated displacement because its contribution grows proportional to the square of time. Common causes of drift include changes in sensor temperature or the structure of the micro-machined parts [13, 4]. A solution is to take advantage of the cyclical nature of walking and divide up the continuous motion into a series of stride cycles (ie. segmentation), resetting integration at the beginning of each new cycle. Resetting treats the new sensor offset as a constant and as long as cycle duration is much shorter than the rate at which the sensor offset is changing, quite accurate results can be achieved. However, resetting introduces a third issue—the initial conditions at the beginning of each integration must be known.

Sabatini and colleagues have demonstrated that it is possible to correctly account for these issues and directly integrate measured accelerations to yield accurate estimates of walking speed [19]. These authors placed an IMU on the top of the foot and resolved the gravitational acceleration component using the gyroscope signal. Integration resetting took advantage of the unique mechanics of the foot during locomotion—that it has zero linear and angular velocity once per stride when the foot is flat—to determine the initial conditions for each new integration. The algorithm was quite accurate with root mean square speed estimation errors of about 5%. While the approach of Sabatini and colleagues is quite useful, it is not always desirable to mount sensors directly on the feet. They may easily move out of the plane of progression, especially during pathological gait, because of the complex motions of the ankle joint during walking [10]. In addition, mounting sensors closer to the knee joint would be more useful for the embedded control of knee-mounted devices such as prostheses, orthoses, exoskeletons and energy harvesters [9, 20, 12, 6].

The purpose of this paper was to study the feasibility of estimating walking speed and slope using a shank-mounted inertial measurement unit. Our approach took advantage of the inverted pendulum-like behavior of the stance leg during walking to identify a new method for segmenting the gait cycle and estimating the initial conditions for integration. To test its accuracy, we compared algorithm speed and slope estimates to known values during walking overground and on a treadmill at a range of speeds and inclines.

2. Methods

2.1. Speed and slope estimation

Shank linear accelerations and angular velocity were measured using a bi-axial accelerometer (Analog Devices ADXL320) and a gyroscope (Analog Devices ADXRS300), respectively. When the shank is vertical with respect to the world coordinate system, the tangential and normal axes of the accelerometer point in the fore-aft and vertical directions, respectively (Figure 1). The gyroscope axis is orthogonal to the plane defined by the tangential and normal axes. Shank angle, θ, is defined as the angle between the normal axis of the accelerometer and the vertical axis of the world coordinate system. As per the right hand rule, positive angular velocity corresponds to a counterclockwise rotation of the shank.

To compute the displacements along the horizontal and vertical world coordinate axes, we first resolved the accelerometer-measured acceleration signals $a_n(t)$ and $a_t(t)$ at time t into component accelerations $a_x(t)$ and $a_y(t)$

in the world coordinate system according to

$$\begin{aligned} a_x(t) &= -a_n(t)\sin\theta(t) + a_t(t)\cos\theta(t) \\ a_y(t) &= a_n(t)\cos\theta(t) + a_t(t)\sin\theta(t) - g, \end{aligned} \tag{1}$$

where $\theta(t)$ is the shank angle, and g is the acceleration due to the gravity (Figure 1). The shank angle $\theta(t)$ was computed by integrating the gyroscope-measured angular velocity $\omega(t)$,

$$\theta(t) = \int_0^t \omega(\tau)d\tau + \theta(0), \tag{2}$$

where $\theta(0)$ is the initial shank angle before integration.

With the resolved acceleration $a_x(t)$ and $a_y(t)$, we computed the associated velocities $v_x(t)$ and $v_y(t)$,

$$\begin{aligned} v_x(t) &= \int_0^t a_x(\tau)d\tau + v_x(0) \\ v_y(t) &= \int_0^t a_y(\tau)d\tau + v_y(0), \end{aligned} \tag{3}$$

where $v_x(0)$ and $v_y(0)$ are the initial horizontal and vertical velocity conditions.

By integrating the velocities $v_x(t)$ and $v_y(t)$, we obtained the horizontal displacement, $s_x(t)$, and vertical displacement, $s_y(t)$,

$$\begin{aligned} s_x(t) &= \int_0^t v_x(\tau)d\tau + s_x(0) \\ s_y(t) &= \int_0^t v_y(\tau)d\tau + s_y(0), \end{aligned} \tag{4}$$

where $s_x(0)$ and $s_y(0)$ are the initial horizontal and vertical positions before the start of integration.

We segmented the continuous walking motion into a series of stride cycles and reset the integration of Equations (2)-(4) at the beginning of each new cycle. Mid-stance shank vertical events—the time in the stance phase when the shank is parallel to the direction of gravity—defined each new stride cycle. The inverted pendulum-like behavior of the stance leg during walking allowed us to identify each mid-stance shank vertical event from a characteristic feature in the gyroscope signal (Figure 2). During the inverted pendulum-like stance phase, the body vaults up and over the stance leg with shank angular velocity negative and slowing down as kinetic energy is exchanged for potential energy [5]. At the shank vertical event, the body center of mass reaches its highest point, potential energy reaches a maximum, and velocity reaches a minimum. The angular velocity of the shank is slowest at this point but then accelerates as the inverted pendulum swings down, exchanging potential energy for kinetic energy. The angular velocity of the shank switches from negative to positive during swing in order to progress the shank forward and return it to the correct orientation at the beginning of the next stance phase. Thus, the characteristic feature for defining mid-stance shank vertical events was the local maximum during the lengthy period of negative angular velocity (Figure 3).

Mid-stance shank vertical is a convenient event to define the initial conditions for integration. By definition, $\theta(0) = 0$ at mid-stance shank vertical thereby providing the initial condition for integrating Equation (2). If the stance leg behaves like an inverted pendulum, $v_y(0) = 0$ at mid-stance shank vertical because the body has reached its maximum height (Equation 3). As the sensor is located much closer to the center of inverted pendulum rotation than that of the center of mass, its horizontal velocity is much smaller than that of the center of mass (Figure 2). We assume, as a first approximation, that $v_x(0) = 0$ at mid-stance shank vertical (Equation 3; c.f. Discussion). The initial conditions for Equation (4) will not affect the estimation results—we set them both equal to zero for simplicity. These initial conditions allowed the integration of Equations (2)-(4) over each gait cycle duration, T, providing a first estimate of horizontal and vertical displacements.

To reduce the estimation error caused by offsets in the acceleration measurements, we assumed zero net acceleration within each stride cycle. While the shank continuously accelerates and decelerates, the average acceleration is zero in each stride cycle during steady state walking. With zero acceleration, the shank horizontal and vertical velocities will be the same at the beginning and at the end of the stride cycle. While the horizontal velocity at the beginning of the stride, $v_x(0)$, equals zero, offsets in the acceleration measurements result in the horizontal velocity at the end of the stride, $v_x(T)$, not being equal to zero. We estimated this mean horizontal acceleration offset, $\bar{a}_x$, as

$$\bar{a}_x = (v_x(T) - v_x(0))/T. \tag{5}$$

The contribution of this offset $\bar{a}_x$ to the estimated horizontal displacement was

$$\bar{s}_x = \frac{1}{2}\bar{a}_x T^2 = \frac{1}{2} T \cdot v_x(T). \tag{6}$$

Similarly, we estimated the mean vertical acceleration offset, $\bar{a}_y$, as

$$\bar{a}_y = (v_y(T) - v_y(0))/T. \tag{7}$$

The contribution of this offset to the estimated vertical displacement was

$$\bar{s}_y = \frac{1}{2}\bar{a}_y T^2 = \frac{1}{2} T \cdot v_y(T). \tag{8}$$

At the end of each gait cycle, we performed a correction on the estimated horizontal and vertical displacement of Equation (4) by subtracting the corresponding offsets from Equations (6) and (8). The corrected horizontal displacement $s'_x(T)$ and vertical displacement$s'_y(T)$ in the gait cycle were calculated as

$$\begin{aligned} s'_x &= s_x(T) - \tfrac{1}{2} T \cdot v_x(T) \\ s'_y &= s_y(T) - \tfrac{1}{2} T \cdot v_y(T), \end{aligned} \tag{9}$$

and the stride length s_T was computed as

$$s_T = \sqrt{(s'_x)^2 + (s'_y)^2}. \tag{10}$$

With the stride length s_T, we computed the average walking speed $V(T)$, in m/s, and slope $\phi(T)$, in percent grade, for each gait cycle as

$$\begin{aligned} V(T) &= s_T / T \\ \phi(T) &= \tfrac{s'_y(T)}{s'_x(T)} \cdot 100. \end{aligned} \tag{11}$$

Before each walking experiment, we calibrated the accelerometer by aligning its axes parallel with gravity (nominal output of 1g) and perpendicular to the gravity (nominal output of 0g) and adjusted the gain and offset accordingly. We performed a single calibration procedure for the gyroscope using a dynamometer (BIODEX II, Biodex Medical Systems, New York) to rotate the device at predefined angular velocities. During the experiment, the sensor signals were digitized (16 bit) at a sample rate of 1 kHz (PCMCIA card NI DAQ 6036E, National Instrument Inc, Austin, TX) and low-pass filtered (Second order, Butterworth, 4 Hz cut-off). The speed and slope estimation algorithms were programmed in Simulink, compiled using Real Time Work-shop and executed in real-time using Real Time Windows Target on a laptop computer (Mathworks, Natick, MA).

2.2. Experimental methods

To test the proposed methods, we performed treadmill and overground walking experiments. Five male and three female subjects (age: 28.0 ± 5.8 years; height: 1.68 ± 0.07; tibia length: 0.41 ± 0.03 m) participated in the treadmill walking experiment. The three female subjects also performed overground walking experiments. All subjects were healthy and exhibited no clinical gait abnormalities. Before the experiments began, volunteers gave their informed consent to participate in accordance with university policy.

After familiarizing the subjects with the experimental protocol and treadmill walking, we collected data at treadmill speeds of $0.8, 1.0, 1.2$, 1.4, 1.6, and 1.8 m/s. At each speed, subjects walked at $-10\%, -5\%, 0\%, 5\%$, and 10% grade. Subjects wore their own walking shoes and athletic clothing. Trials were $90s$ in duration. During all trials, an IMU was attached with athletic tape directly onto the calf and parallel to the sagittal plane. The center of the IMU was positioned midway between the knee and ankle along the longitudinal axis of the shank. To identify the effects of sensor location on gait parameter estimation, we performed additional experiments with the center of the IMU unit positioned at 25% (proximal), and 75% (distal) along the longitudinal axis. In these trails, subjects walked at the full range of speeds but only on the level grade. During the overground experiments, subjects completed two trials of walking along a straight 100 meter long course at their preferred walking speed with the IMU in the middle position.

2.3. Data analysis

For each treadmill walking trial, we calculated the mean walking speed and slope by averaging the stride-by-stride data from the last 60s of each trial. Estimation error at a given speed and slope was calculated as the difference between the estimated speed or slope and the actual treadmill value. Within a condition, we averaged across subjects to determine the mean estimation error (Mean) and standard derivation (S.D.). We also calculated the root mean square error (RMSE) of the speed estimates as RMSE = $\sqrt{\sum (\text{estimated-actual})^2/N}$ (N is the number of samples). For each slope, we calculated the RMSE between eight subjects across six speeds ($N = 48$). For each individual walking speed, the RMSE was calculated across five slopes within eight subjects ($N = 40$). The overall RMSE was calculated across all of the testing speeds and slopes within eight subjects ($N = 240$). The effects of walking speed, slope and sensor location on speed and slope estimation error were tested using repeated-measures ANOVA, with $P < 0.05$ considered statistically significant. For overground walking trials, we computed the mean and RMSE of the estimated walking distance.

3. Results

The proposed speed estimation method accurately estimated walking speed. Figure 4 presents typical data from a single subject during level walking. For this representative subject, speed and slope are estimated accurately and with low variability. This pattern holds across the eight measured subjects as summarized in Figure 5 and Table 1. While actual speed did not affect the speed estimation error during level walking ($P = 0.065$), the algorithm tended to slightly overestimate at slow speeds and underestimate at fast speeds. Estimation errors were nevertheless small with the largest being -0.10 m/s at 1.8 m/s. Walking slope had a systematic effect on estimated speed ($P = 0.04$). In general, the speed estimation algorithm was accurate across speeds and slopes—the RMSE for speed estimation was only 7%. The accuracy of speed estimation resulted in accurate distance estimation. The mean value of the estimated distance covered in the six overground walking trials was 96.5 ± 2.0 m equating to a RMSE of 4%.

Unlike the speed estimation method, the proposed slope estimation method was not accurate (Figure 6). While the estimated slope for level walking, averaged across all walking speeds, was close to zero (-2.3%), variability between subjects was high (4.2% S.D.). For level walking, the slope estimation error was not affected by walking speed ($P = 0.41$). Actual slope had a systematic effect on estimated slope ($P = 9.8e-7$), with the method tending to underestimate both the degree of incline and the degree of decline. At the steepest decline of -10% grade and the highest walking speed of 1.8 m/s, the algorithm estimated a positive slope of 5% grade, resulting in the largest absolute estimation error.

4. Discussion

Our results indicate that a shank-mounted inertial measurement unit can provide accurate estimates of walking speed across a wide range of speeds and slopes. This approach leveraged walking's inverted pendulum-like behavior to define individual gait cycles based on mid-stance shank vertical events and estimate the initial conditions for integration. The algorithm worked well across speeds and slopes yielding a root mean square speed estimation error of only 7%.

The position of the sensor along the shank affected speed estimation results (Figure 7). To determine the initial condition for integrating the sensor horizontal acceleration, we assumed a zero sensor horizontal velocity at mid-stance shank vertical (Equation 3). Any deviation of the actual initial horizontal velocity from zero would result in the same amount of offset in the estimated horizontal speed. Because the shank rotates about the ankle joint at the mid-stance shank vertical event, the absolute value of the initial horizontal velocity $v_x(0)$ is approximately equal to the product of the angular velocity omega of the shank and the distance of the sensor to the ankle joint (Figure 2). At the mid-stance shank vertical event, the shank angular velocity reached a non-zero local maximum resulting in a positive nonzero initial horizontal velocity (Figure 3). The speed estimation algorithm underestimated walking speed, and the underestimation became larger at faster walking speeds, because the shank retained a greater angular velocity, and therefore a larger initial horizontal velocity, at the peak of the inverted pendulum arc. As expected, a more proximal

Table 1: Speed estimation errors at different speeds and slopes

		Speed (m/s)						
Slope		0.8	1.0	1.2	1.4	1.6	1.8	RMSE
−10%	abs.	0.01±0.08	−0.03 ± 0.10	−0.01 ± 0.10	−0.04 ± 0.10	−0.06 ± 0.11	−0.16 ± 0.11	0.12
	pct.	0.01 ±0.1	−0.03 ± 0.1	−0.01 ± 0.08	−0.03 ± 0.07	−0.03 ± 0.07	-0.09 ±0.06	0.09
−5%	abs.	0.04 ± 0.07	0 ± 0.06	0.04±0.06	0±0.07	−0.02 ± 0.07	−0.09 ± 0.08	0.08
	pct.	0.05 ± 0.09	0 ± 0.06	0.03 ±0.05	0 ±0.05	−0.02 ± 0.05	−0.05 ± 0.04	0.06
0%	abs.	0.01 ± 0.07	−0.03 ± 0.06	−0.03 ± 0.06	−0.05 ± 0.06	−0.05 ± 0.07	−0.10 ± 0.07	0.08
	pct.	0.02 ± 0.09	−0.03 ± 0.06	−0.03 ± 0.05	−0.03 ± 0.04	−0.03 ± 0.04	−0.06 ± 0.04	0.06
5%	abs.	0.02 ± 0.06	−0.02 ± 0.03	0.01 ± 0.03	−0.02 ± 0.05	−0.01 ± 0.04	−0.06 ± 0.04	0.05
	pct.	0.02±0.08	−0.02 ± 0.03	0.01 ± 0.02	−0.01 ± 0.03	0 ± 0.02	−0.03 ± 0.02	0.04
10%	abs.	0.10 ± 0.05	0.06 ± 0.05	0.10 ± 0.05	0.05 ± 0.03	0.06 ± 0.03	−0.01 ± 0.05	0.08
	pct.	0.12 ± 0.06	0.06 ± 0.05	0.08 ± 0.04	0.04 ± 0.02	0.04 ± 0.02	−0.01 ± 0.03	0.08
RMSE	abs.	0.08	0.07	0.08	0.07	0.08	0.12	0.08
	pct.	0.10	0.07	0.06	0.05	0.05	0.07	0.07

Absolute estimation error(abs.), percentage estimation error (pct.) at different speed and slope are shown.
Values are means $\pm S.D.$, $N = 8$.

sensor placement resulted in an even larger degradation in estimation error at faster speeds. Speed estimation error in the distal sensor was independent of speed but suffered from a small but constant overestimation. The tradeoff between the underestimation from the middle sensor and overestimation from the distal sensor suggests that the ideal IMU location to minimize speed estimation error would be between the middle and distal sensor locations.

Our approach failed to provide accurate slope estimation by consistently underestimating both positive and negative slopes. These inaccuracies appear to arise, at least in part, from limitations of using an inverted pendulum model to predict shank vertical events during slope walking. During incline walking, the COM kinetic energy reaches its minimum prior to the COM gravitational potential energy reaching its maximum [8]. In the context of our method, this implies that the local maximum of shank angular velocity occurs prior to the stance leg reaching its vertical position during incline walking. The order of the COM energy extrema is reversed during decline walking [8] suggesting that the local maximum of shank angular velocity occurs after the stance leg reaching its vertical position. Non-zero shank angles at predicted shank vertical events results in positive and negative initial vertical velocities during incline and decline walking, respectively. Our method assumes that the initial vertical velocity is zero (Equation 3), underestimating the actual vertical speed and, consequently, underestimating slope. Because grade is calculated as the ratio between the estimated vertical displacement and the estimated horizontal displacement (Equation 11), small absolute errors in vertical speed can have a large effect on estimated slope at small slope angles. There is a much less pronounced effect of small absolute errors on estimated speed (Equation 11) explaining why accurate speed estimation can be accompanied by poor slope estimation.

While not suitable for estimating slope, the present method appears to provide a greater accuracy at estimating speed than the most accurate indirect method and without requiring subject-specific calibration [15, 1, 21]. The present accuracy is roughly comparable to that achieved by Sabatini and colleagues who, like us, used direct integration of accelerations but from a sensor mounted to the foot [19]. That accurate results can be achieved with either method allows for flexibility in sensor positioning. This may be of great benefit for integrating sensors directly into a knee-mounted device, such as an energy harvester [6], or for estimating speed in walking with abnormal foot motion, such as the equinus gait often observed in children with cerebral palsy [7].

Acknowledgements

This research was partially supported by an MSFHR Postdoctoral Trainee award to Q. Li, a Queen's ARC grant to Q. Li, and an MSFHR Scholar Award, a CIHR New Investigator Award, and CIHR Operating Grant 159895 to JMD.

References

[1] Aminian, K., Najafi, B., Bula, C., Leyvraz, P. F., Robert, P., 2002. Spatio-temporal parameters of gait measured by an ambulatory system using miniature gyroscopes. Journal of Biomechanics 35 (5), 689–699.

[2] Aminian, K., Rezakhanlou, K., De Andres, E., Fritsch, C., Leyvraz, P., Robert, P., 1999. Temporal feature estimation during walking using miniature accelerometers: an analysis of gait improvement after hip arthroplasty. Medical and Biological Engineering and Computing 37 (1), 686–691.

[3] Andriacchi, T., Ogle, J., Galante, J., 1977. Walking speed as a basis for normal and abnormal gait measurements. Journal of Biomechanics 10 (4), 261–8.

[4] Boonstra, M., van der Slikke, R., Keijsers, N., van Lummel, R., de Waal Malefijt, M., Verdonschot, N., 2006. The accuracy of measuring the kinematics of rising from a chair with accelerometers and gyroscopes. Journal of Biomechanics 39 (2), 354–358.

[5] Cavagna, G., Heglund, N., Taylor, C., 1977. Mechanical work in terrestrial locomotion: two basic mechanisms for minimizing energy expenditure. American Journal of Physiology- Regulatory, Integrative and Comparative Physiology 233 (5), 243–261.

[6] Donelan, J. M., Li, Q., Naing, V., Hoffer, J. A., Weber, D. J., Kuo, A. D., 2008. Biomechanical energy harvesting: generating electricity during walking with minimal user effort. Science 319 (5864), 807–10.

[7] Goldstein, M., Harper, D., 2001. Management of cerebral palsy: equinus gait. Developmental Medicine and Child Neurology 43 (08), 563–569.

[8] Gottschall, J., Kram, R., 2006. Mechanical energy fluctuations during hill walking: the effects of slope on inverted pendulum exchange. Journal of Experimental Biology 209 (24), 4895.

[9] Herr, H., Wilkenfeld, A., 2003. User-adaptive control of a magnetorheological prosthetic knee. Industrial Robot: An International Journal 30 (1), 42–55.

[10] Jasiewicz, J. M., Allum, J. H., Middleton, J. W., Barriskill, A., Condie, P., Purcell, B., Li, R. C., 2006. Gait event detection using linear accelerometers or angular velocity transducers in able-bodied and spinal-cord injured individuals. Gait Posture 24 (4), 502–9.

[11] Judge, J., Underwood, M., Gennosa, T., 1993. Exercise to improve gait velocity in older persons. Archives of physical medicine and rehabilitation 74 (4), 400–406.

[12] Kazerooni, H., Steger, R., Huang, L., 2006. Hybrid Control of the Berkeley Lower Extremity Exoskeleton (BLEEX). The International Journal of Robotics Research 25 (5-6), 561.

[13] Luinge, H., Veltink, P., 2004. Inclination measurement of human movement using a 3-D accelerometer with autocalibration. IEEE Transactions on Neural Systems and Rehabilitation Engineering 12 (1), 112–121.

[14] Maki, B., 1997. Gait changes in older adults: predictors of falls or indicators of fear. J Am Geriatr Soc 45 (3), 313–20.

[15] Miyazaki, S., 1997. Long-term unrestrained measurement of stride length and walking velocity utilizing a piezoelectric gyroscope. Ieee Transactions on Biomedical Engineering 44 (8), 753–759.

[16] Moe-Nilssen, R., Helbostad, J., 2004. Estimation of gait cycle characteristics by trunk accelerometry. Journal of biomechanics 37 (1), 121–126.

[17] Pappas, I., Popovic, M., Keller, T., Dietz, V., Morari, M., 2001. A reliable gait phase detection system. IEEE Transactions on neural systems and rehabilitation engineering 9 (2), 113–125.

[18] Richards, C., Malouin, F., Wood-Dauphinee, S., Williams, J., Bouchard, J., Brunet, D., 1993. Task-specific physical therapy for optimization of gait recovery in acute stroke patients. Arch Phys Med Rehabil 74 (6), 612–20.

[19] Sabatini, A. M., Martelloni, C., Scapellato, S., Cavallo, F., 2005. Assessment of walking features from foot inertial sensing. IEEE Trans Biomed Eng 52 (3), 486–94.

[20] Weinberg, B., Nikitczuk, J., Patel, S., Patritti, B., Bonato, P., Canavan, P., 2007. Design, Control and Human Testing of an Active Knee Rehabilitation Orthotic Device, 4126–4133.

[21] Zijlstra, W., Hof, A. L., 2003. Assessment of spatio-temporal gait parameters from trunk accelerations during human walking. Gait & Posture 18 (2), 1–10.

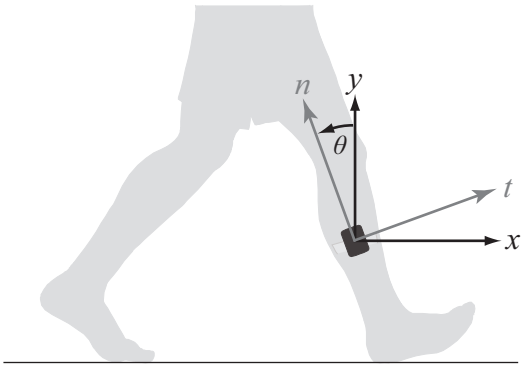

Figure 1: Sensor configuration. An inertial measurement unit (IMU) is attached to the shank in the sagittal plane on the lateral side. The normal acceleration a_n is measured along the n direction, and the tangential acceleration a_t is measured along the t direction. The arrows indicate positive axes for the corresponding sensor measurements. The world coordinate is defined by the x and y axes, and the vertical axis y extends in a direction parallel to gravity.

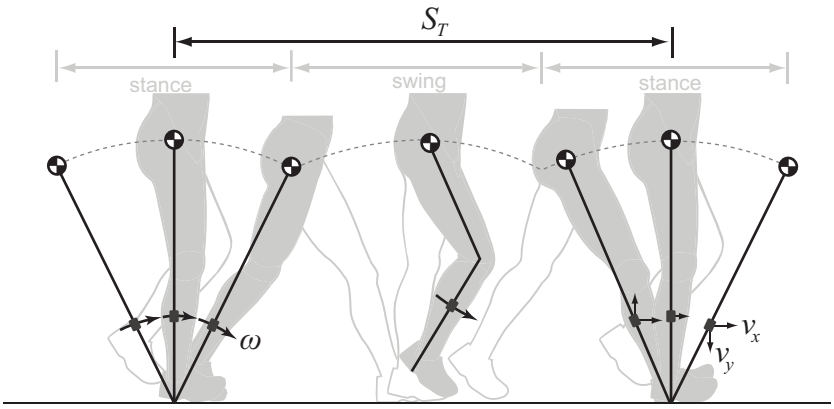

Figure 2: Due to the inverted pendulum-like behavior of leg during stance, the angular velocity of the shank (ω; left side arrows) first slows down and then speeds up with its minimum speed occurring at mid-stance shank vertical. Consequently, the IMU horizontal and vertical velocities (v_x and v_y; right side arrows) are approximately zero at mid-stance. Shank angular velocity switches from negative to positive during swing in order to progress the shank forward and return it to the correct orientation at the beginning of the next stance phase. S_T is the stride length between two mid-stance shank vertical events.

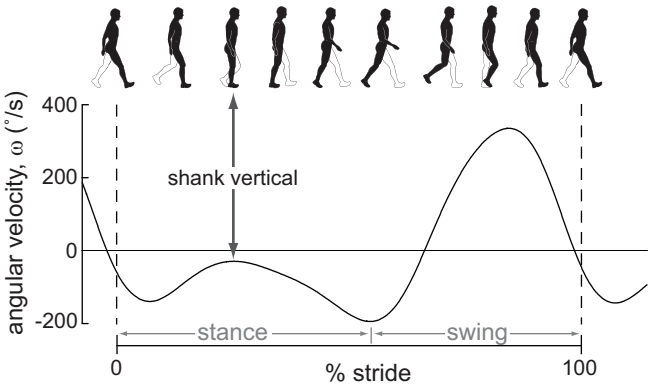

Figure 3: Shank configuration and filtered angular velocity, ω. At mid-stance shank vertical, the angular velocity of the shank reaches a local maximum with a value close to zero.

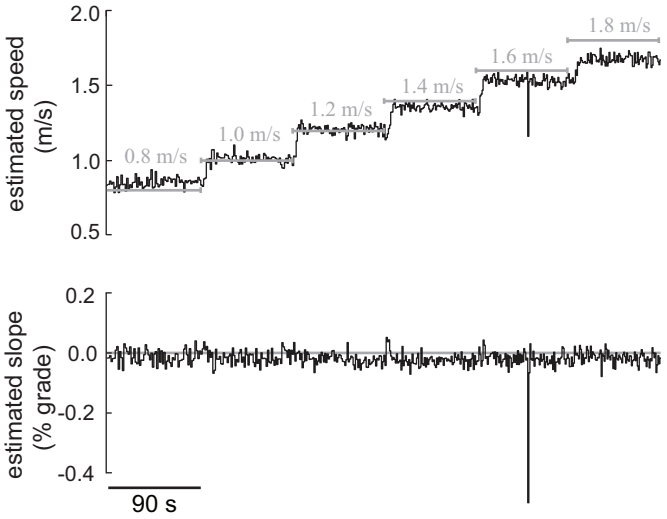

Figure 4: Estimated speed and slope from a representative subject during level walking at treadmill speeds ranging from 0.8 m/s to 1.8 m/s.

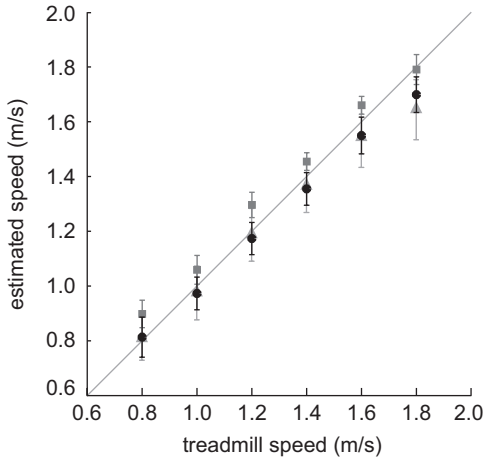

Figure 5: Estimated speeds during −10% (▲), 0% (●) and 10% (■) grade walking. The solid grey line is the line of identity where the estimated speed equals the treadmill speed. Values shown are means± S.D., $N = 8$.

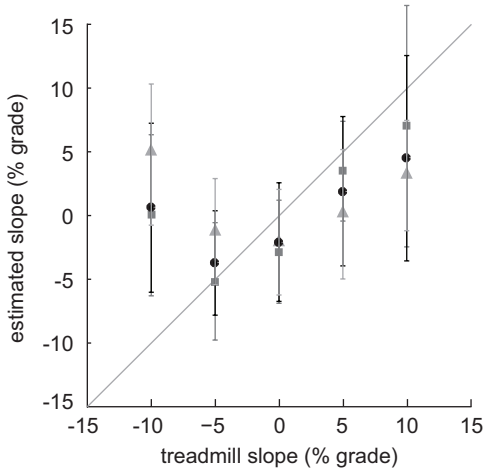

Figure 6: Estimated slopes during walking speeds at 0.8 m/s (■), 1.2 m/s (●) and 1.8 m/s (▲). The solid grey line is the line of identity where the estimated slope equals the treadmill slope. Values shown are means± S.D., $N = 8$.

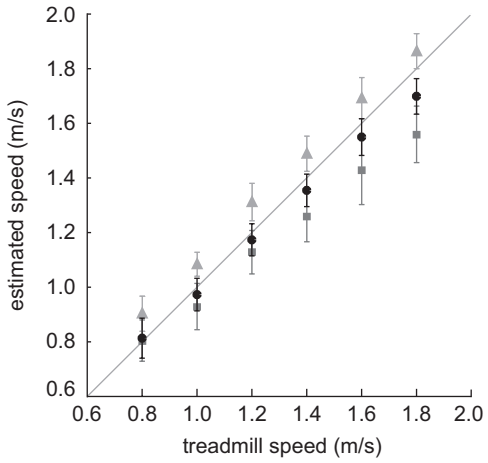

Figure 7: Estimated speeds during level walking with the sensor locations at placed along the longitudinal axis of the shank at proximal (■), middle (●) and distal (▲) locations. The solid grey line is the line of identity where the estimated speed equals the treadmill speed. Values shown are means± S.D., $N = 8$.